Electron Emission from Individual Graphene Nanoribbons Driven by Internal Electric Field

Xianlong Wei,[†,‡,*] Yoshio Bando,[‡] and Dmitri Golberg[‡,*]

[†]International Center for Young Scientists (ICYS) and [‡]International Center for Materials Nanoarchitectonics (MANA), National Institute for Materials Science (NIMS), Namiki 1-1, Tsukuba, Ibaraki, 305-0044, Japan

ABSTRACT

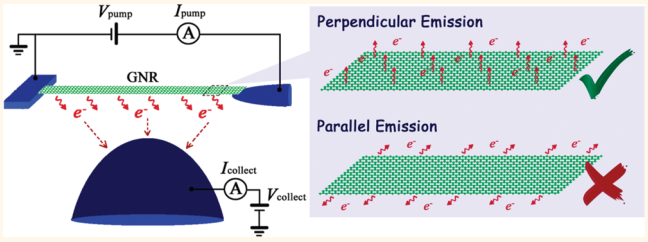

Electron emission from individual graphene nanoribbons (GNRs) driven by an internal electric field was studied for the first time inside a high resolution transmission electron microscope equipped with a state-of-art scanning tunneling microscope sample holder with independent twin probes. Electrons were driven out from individual GNRs under an internal driving voltage of less than 3 V with an emission current increasing exponentially with the driving voltage. The emission characteristics were analyzed by taking into account monatomic thickness of GNRs. While deviating from the two-dimensional Richardson equation for thermionic emission, they were well described by the recently proposed by us phonon-assisted electron emission model. Different from widely studied field electron emission from graphene edges, electrons were found to be emitted perpendicularly to the atomic graphene surfaces with an emission density as high as 12.7 A/cm^2. The internally driven electron emission is expected to be less sensitive to the microstructures of an emitter as compared to field emission. The low driving voltage, high emission density, and internal field driving character make the regarded electron emission highly promising for electron source applications.

KEYWORDS: graphene nanoribbon · phonon-assisted electron emission · thermionic emission · one-atom-thick surface · *in situ* measurement

Graphene, a single atomic layer of graphite, has attracted great research interests in recent years due to its fascinating physical properties and promising applications. Considering its monatomic thickness, excellent electrical and thermal conductivities, and outstanding mechanical properties, graphene is thought to be a promising material for electron emitters, and electron emission from graphenes has indeed been intensively studied. Graphene films have been demonstrated to exhibit outstanding field electron emission performance with low turn-on and threshold electric fields, high emission density and good stability comparable to, or even better, than those of carbon nanotube (CNT) films.[1−6] For example, a turn-on electric field as low as 0.6 V/μm has been demonstrated for N-doped graphene films by Palnitkar *et al.*[4] Field electron emission characteristics of individual graphenes were studied by using nanoprobes as anodes,[7−9] and were found to deviate from conventional Fowler-Nordheim (FN) theory, but were well described by the theoretical equations taking into account the two-dimensional (2D) nature of graphenes.[7] Well-aligned graphene field emission arrays have also been successfully fabricated aiming at field emission display applications.[10] To date, all studies of electron emission from graphenes have mainly been focused on their field emission characteristics.[1−10] However, in field emission, electrons are pulled out from a sharp solid surface by using an extremely high external electric field with a local strength as high as ~10^9 V/m,[11] and usually a high external voltage of the order of 10^2 V is needed.[12] Moreover, electron emission under the pulling force of an external electric field makes field emission highly sensitive to the local field enhancement factor and thus to a given microstructure or even atomic structure at the emission sites,[12,13] which is difficult to be controlled. Also, the field electron emitters have to work in ultrahigh vacuum, and their fabricating cost becomes too high. Since the edge structures of graphenes are still uncontrollable, the high emission sensitivity to the microstructure status of an emitter makes it difficult to fabricate a single graphene field emitter, or an emitter array with the desired properties in a reproducible manner, similarly to the same drawback in the case of CNT field emitters.[13] Those reasons may keep

* Address correspondence to WEI.Xianlong@nims.go.jp, weixl@pku.edu.cn, GOLBERG.Dmitri@nims.go.jp.

Received for review October 30, 2011 and accepted November 25, 2011.

Published online November 25, 2011
10.1021/nn204172w

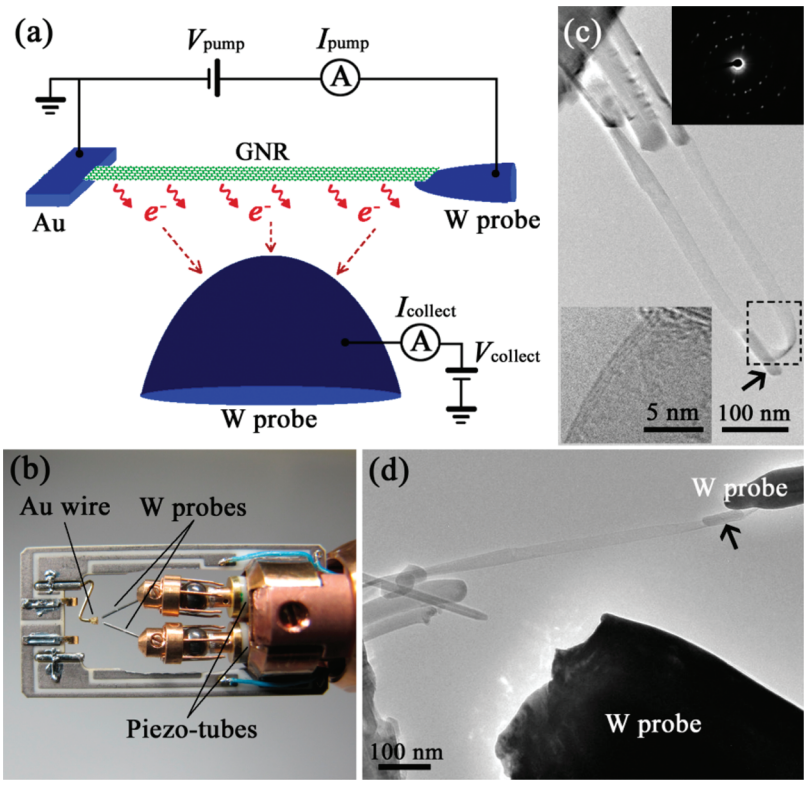

Figure 1. (a) Schematic drawing of the three-terminal measurement setup. (b) A photo image of the sample holder with individually piezo-driven twin probes. (c) TEM image of a typical GNR under study. The bend in the framed area clearly shows that the structure is a ribbon. The insets are a high resolution TEM image (bottom-left) and an electron diffraction pattern (upper-right). The elliptical shape of diffraction spots/rings distribution is a result of the GNR tilt with respect to the incident electron beam. (d) TEM image of a three-terminal measurement setup constructed on the GNR shown in panel c. The arrowed dark contrast particle serves as a marker in panels c and d that indicates the exact way of the final ribbon placement between the electrodes.

possible graphene field emitters far away from the real market. Therefore, it is highly desirable to develop graphene electron emitters working at a low electric field/voltage and with a low sensitivity to the emitter micro- and/or nanostructure.

In addition to being highly promising for use as electron emitters, one-atom-thick graphene can be an ideal system for studying the basic electron emission laws at low dimensions. The one-atom thickness enables all electrons in graphene to always be at its boundary with vacuum. However, in a three-dimensional (3D) bulk solid, only the electrons near the surfaces (those electrons are only the marginal part of all electrons in a 3D solid) are at such a boundary. Since only through passing that boundary can electrons be emitted and only some of them (locating very near to the boundary) can be emitted immediately, the existing boundary-only electrons in graphene make the graphene's electron emission characteristics, and even its mechanisms, quite different from those of a 3D solid. However, until now, there have been very few studies concerning the electron emission characteristics and the emission mechanisms associated with the graphene's low dimensionality.[7,14]

Herein, electron emission from individual graphene nanoribbons (GNRs) driven by an internal electric field is studied for the first time inside a high resolution transmission electron microscope (TEM). The internal electric field driving character results in much lower emission sensitivity to the emitters' structures. Electrons were driven out from individual GNRs by using an internal electric field with a strength of only 10^6 V/m and a driving voltage of less than 3 V, which are two or three orders of magnitude lower than those needed for the standard field emission. On the basis of the careful analysis of the emission currents measured at different driving voltages, and by taking into account the monatomic thickness of GNRs, the observed electron emission was attributed to phonon-assisted electron emission (PAEE), a recently proposed by us mechanism peculiar to the monatomic surfaces.[15] Different from widely studied field electron emission from graphene edges,[1−10,14] electrons were found to be emitted perpendicularly to the graphene surfaces with an emission density as high as 12.7 A/cm^2.

RESULTS AND DISCUSSION

To obtain intrinsic electron emission characteristics of GNRs associated with their low dimensionalities,

measurements on individual GNRs are desired. Herein, we adopted a three-terminal measurement setup, schematically shown in Figure 1a, and studied internal electric field driven electron emission from individual GNRs. A GNR sample was prepared by suspending an individual GNR between the two metal electrodes (a W probe and an Au wire edge). A driving voltage (V_{pump}) was then applied to the GNR to pump up electrons and drive electron emission from it. At the same time, a collecting voltage ($V_{collect}$) was applied to the third electrode (a W probe) located near the middle of the nanoribbon to collect electrons emitted from it. Emission current ($I_{collect}$) was measured at different V_{pump} and $V_{collect}$.

The experiments were performed *in situ* inside a high resolution TEM equipped with a state-of-art sample holder with piezo-tube driven twin STM probes (Figure 1b), which makes it possible to construct a three-terminal measurement setup on an individual GNR, as shown in Figure 1a. Figure 1c shows the TEM image of a typical GNR with three atomic layers. The clear fringes in the high resolution TEM image and (0002) spots in the diffraction pattern indicate that the GNR has closed edges in agreement with most observations of graphenes,[16] and that it may structurally resemble a fully collapsed nanotube.[17] Figure 1d displays a three-terminal measurement setup constructed on the GNR shown in Figure 1c. For constructing the measurement setup, one end of the GNR in Figure 1c was first disconnected from its basement support using an electron beam as a cutter, followed by delicate nanomanipulations aimed at its reconnection to the W probe. The *in situ* TEM measurements enable us to straightforwardly correlate the electron emission characteristics of a GNR with its structures.

Figure 2 shows the measurement results from a 1.17 μm long and 15.5 nm wide GNR (inset of Figure 2a). The two-terminal $I_{pump}-V_{pump}$ curve, shown in Figure 2a, exhibits a typical electron transport character of GNRs. When V_{pump} was higher than a threshold value of *ca.* 2.4 V, an emission current ($I_{collect}$) collected by the collecting probe became measurable. We measured $I_{collect}-V_{collect}$ curves at different V_{pump}, between 2.50 and 2.90 V, with an 0.01 V interval, and representative curves for the 0.05 V intervals are shown in Figure 2b. All $I_{collect}-V_{collect}$ curves exhibit a fast increasing regime followed by a slow increasing stage. The fast increasing regime is attributed to the space charge regime (the left side from the dashed line in Figure 2b) where electrons are retarded by space charges, while the slow increasing stage is the accelerating field regime (the right side from the dashed line in Figure 2b) where emission current increase originates from a decrease of the surface barrier caused by an $V_{collect}$ increase.[18]

It can be seen from Figure 2b that an emission current ($I_{collect}$) also increases with V_{pump} for a given $V_{collect}$.

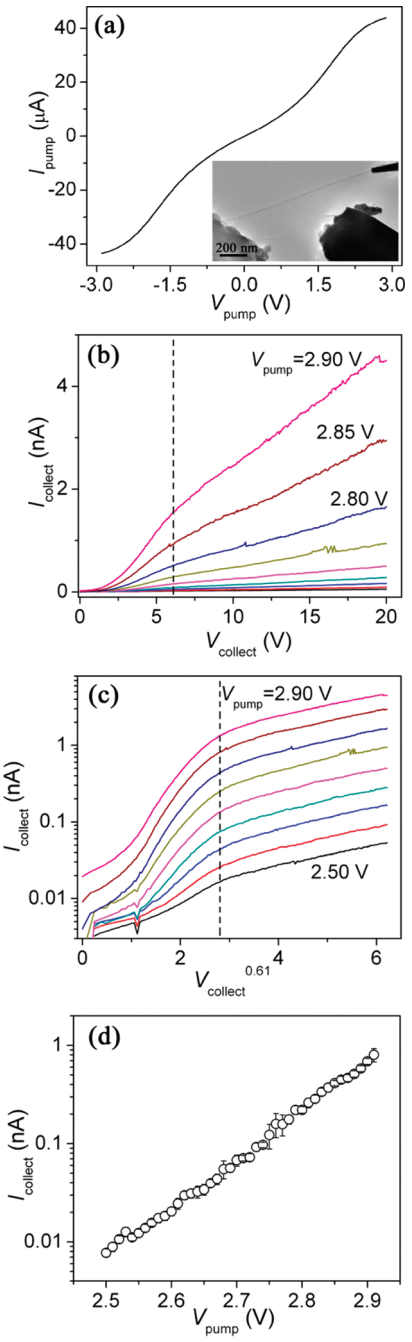

Figure 2. (a) Two-terminal transport characteristics ($I_{pump}-V_{pump}$ curve) of a 1.17 μm long and 15.5 nm wide graphene nanoribbon. The inset is a TEM image showing the measurement on the GNR. (b) $I_{collect}-V_{collect}$ curves of the GNR measured at different V_{pump}, from 2.50 to 2.90 V, with an interval of 0.05 V. (c) Replotted $I_{collect}-V_{collect}$ curves in an exponential scale. The x coordinate is $V_{collect}^{0.61}$ with $V_{collect}$ having a unit of volts. The left side of the dashed lines in panels b and c corresponds to the space charge regime, while the right side is the accelerating field regime. (d) $I_{collect}-V_{pump}$ plot of the nanoribbon at zero collecting voltage obtained through extrapolating $I_{collect}-V_{collect}$ curves in panel c.

This enables us to exclude field emission or external electric field pulling electron emission from the possible mechanisms responsible for the measured electron emission. Since the voltage difference between the

GNR and the collecting probe will decrease if V_{pump} increases and $V_{collect}$ is fixed, the strength of external collecting electric field will decrease with V_{pump} for a given $V_{collect}$. Thus the increase of $I_{collect}$ with V_{pump} for a given $V_{collect}$ indicates that a larger emission current is measured at a lower external collecting electric field, which contradicts the field emission. Therefore, some internal drive by an electric field or heat should be responsible for the observed electron emission.

The exponential law between the emission current and the height of surface barrier has been well established for the mechanisms other than field emission, and $I_{collect}-V_{collect}$ curves in the accelerating field regime can be described by a formula: $\ln I_{collect} = \ln I^0_{collect} + \alpha V^{\beta}_{collect}$,[15,18] where $I^0_{collect}$ is the emission current at zero collecting voltage, and α and β are constants. The $I_{collect}-V_{collect}$ curves in Figure 2b were replotted in exponential scale (Figure 2c). It is clearly seen that $\ln I_{collect}$ increases linearly with $V^{0.61}_{collect}$ in accelerating field regime with almost the same slope (α) for all the curves. So, $I_{collect}-V_{collect}$ curves in Figure 2b can be remarkably well fitted using the formula with $\beta = 0.61$ in the accelerating field regime. By extrapolating the $I_{collect}-V_{collect}$ curves in this regime using this formula, we can get $I^0_{collect}$ corresponding to each V_{pump} as shown in Figure 2d. It is apparent that the emission current at zero collecting voltage increases exponentially by 2 orders of magnitude, from ~0.01 nA to ~1 nA, when the driving voltage (V_{pump}) increases for only 0.4 V. Electrons were driven out from the GNR under the driving voltage of less than 3 V, which corresponds to an internal driving electric field of only $\sim 10^6$ V/m. As compared to a local strength of the external electric field of *ca.* 10^9 V/m and an external pulling voltage of the order of 10^2 V required for field emission,[11,12] it is demonstrated herein that two or three orders lower internal electric field and driving voltage can drive the electron emission from individual GNRs. The above-described electron emission characteristics were reproducible for several GNRs. The representative results obtained from another 680 nm long and 35.3 nm wide GNR can also be found in the Supporting Information.

Now we focus on the possible mechanisms responsible for the electron emission from GNRs. One atom thickness enables all electrons in a GNR to always be at its boundary with vacuum. The only-boundary electrons in GNRs, or any other 2D solids, make their electron emission characteristics quite different from those of a 3D solid. As for electron emission from a 3D solid, it can only take place in one way; that is, the electron emission from the 2D surfaces of the bulk. However, as schematically shown in Figure 3, for electron emission from a 2D solid, it can take place in two quite different ways: parallel emission from one-dimensional (1D) edges (Figure 3a) and perpendicular emission from 2D surfaces (Figure 3b). The former way shares the same physical pictures as the electron emission from 2D surfaces of a 3D solid, whereas the latter one is an additional pathway peculiar to electron emission from a 2D solid and associated with its low dimensionality. The two ways are also associated with different emission mechanisms. Conventional field emission and thermionic emission from a 2D solid take place in the former way,[11,18] whereas recently proposed phonon-assisted electron emission takes place in the latter way.[15] Which way and which mechanism dominate the presently measured electron emission from GNRs is about what we are concerned now.

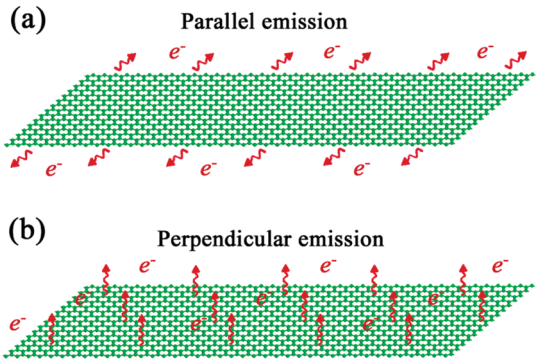

Figure 3. Schematic drawing of the two ways of electron emission from a 2D solid: (a) parallel emission from 1D edges and (b) perpendicular emission from 2D surfaces.

Since field emission has been excluded above, we will first discuss thermionic emission as a possible mechanism responsible for the measured electron emission from GNRs. According to its physical picture, thermionic emission from a GNR takes place in a parallel way from its 1D edges,[18,19] as schematically shown in Figure 3a, just in the same way as for the widely studied field emission from graphenes.[1−10] The 2D Richardson equation should be adopted to calculate the line emission density: $J_{th}(T) = AT^{3/2} \exp(-W/k_BT)$,[19] where T is temperature, $W = 4.7$ eV is work function of graphene,[20] and $A = (2k_B)^{3/2}(\pi m)^{1/2}h^{-2}e$ is the constant with m being the mass of electrons, e being the electron charge, h being the Plank constant and k_B being the Boltzmann constant. For each measured emission current ($I_{collect}$) in our experiments, the corresponding line emission density from the 1D edges of a single graphene layer can be calculated using an equation: $J_L = I_{collect}/(nL)$; here L is the GNR length, $n = 4$ is a factor taking into account two outermost graphene layers for a multilayered GNR with closed edges, and two 1D edges for each layer. Figure 4a shows the calculated line emission density at different V_{pump} based on the emission current in Figure 2d, and the required average temperature of the GNR for the obtained line emission density according to the 2D Richardson equation. It can be seen that, if the measured emission currents are resulted from the thermionic emission, the required average temperature of the nanoribbon should be as

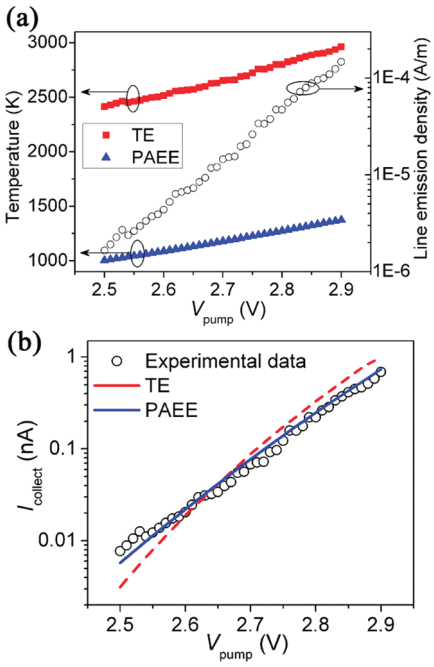

Figure 4. (a) Calculated line emission density (black open circles) corresponding to the emission current in Figure 2d by assuming parallel electron emission from 1D edges of the GNR, and the required temperature (red squares) for the line emission density according to the 2D Richardson equations. (b) The fitting results of the experimental $I_{collect}-V_{pump}$ curve in Figure 2d according to thermionic emission (TE) model and phonon-assisted electron emission (PAEE) model. The theoretical curve (blue solid line) of PAEE model corresponds to the following parameters' values: $R_C = 20$ kΩ, $R_{th} = 0.5 \times 10^7$ K/W, $k_0 = 1400$ W/mK, $W = 5.15$ eV. The values of other parameters needed in the calculation are the same as those in ref 15, except that a phonon lifetime of 1.2 ps was used here. The corresponding temperature of the theoretical curve is shown in panel a using blue triangle symbols.

high as ~3000 K when V_{pump} = 2.9 V. So, the peak temperature at the middle point of the GNR may exceed ~3400 K, if a parabolic temperature profile along the nanoribbon is assumed. At such high temperature, the GNR is expected to experience severe structural changes and even a complete failure,[21] and it is impossible to obtain so stable emission characteristics as those shown in Figure 2.

To further test thermionic emission as a possible mechanism, we tried to simulate the exponential law between the emission current and pumping voltage in Figure 2d according to the thermionic emission model. Assuming a thermal conductivity in the form of $k = k_0(T_0/T)$, where k_0 is the thermal conductivity at room temperature (T_0 = 300 K), the temperature profile of a GNR under Joule-heating at a specific couple of I_{pump} and V_{pump} in Figure 2a can be written as $T_x = T_c \exp[-(p/(2k_0T_0A))(x^2 - Lx)]$,[22] where x is a coordinate along the nanoribbon axis, $p = (I_{pump}V_{pump} - I^2_{pump}R_c)/L$ is the Joule-heating power per unit length and R_c is the contact resistance, A is the cross-sectional area of the GNR, and $T_c = T_0 + R_{th}pL/2$ is the temperature at its two ends where R_{th} is the thermal resistance at contacts. Therefore, a thermionic emission current from a multilayered GNR can be calculated as: $I_{th} = n\int_0^L J_{th}(T_x)\,dx$. By using R_c, R_{th} and k_0 as fitting parameters, we can fit the $I_{collect}-V_{pump}$ curve in Figure 2d according to the thermionic emission model. However, the experimental curve cannot be properly fitted in the frame of the thermionic emission model (Figure 4b). The failure of such fitting, together with the extremely high calculated temperature needed for thermionic emission (Figure 4a), indicates that the observed electron emission from GNRs cannot be attributed to the regarded mechanism.

Another possible mechanism responsible for the observed electron emission is phonon-assisted electron emission,[15] where the electrons are emitted perpendicularly to the 2D graphene atomic surfaces (Figure 3b). Actually, PAEE from GNRs has been predicted in theory.[15] According to phonon-assisted electron emission, when an internal electric field forms after applying a driving voltage, electrons are transported along GNR under the drive of electric force; due to the absorption of forward scattering phonons, electrons can accumulate the energy obtained from the electric field and keep their moving direction when they are scattered by phonons, and thus can be continuously accelerated by electric field until they overcome the surface barrier and are emitted perpendicularly to the one-atom-thick graphene surface. Thus electrons obtain the energy needed to overcome the surface barrier from the inner electric field which drives the regarded electron emission.

Here, we adopted the theoretical model, proposed earlier to calculate PAEE from a CNT,[15] to simulate the presently measured emission current from a GNR. In fact, the latter may be considered as an unfolded CNT. In the model, electrons near the Fermi level of a CNT shell are assumed to be confined in a one-atom-thick quantum well and their distribution function evolves with time according to the coupled Boltzmann equations of both electrons and phonons. Electrons are assumed to break through the confinement of the quantum well and escape from tube shell into vacuum once their energy becomes higher than the depth of the quantum well. The phonon-assisted emission current from a GNR was calculated using a formula: $I_{PAEE} = 2w\int_0^L J_{PAEE}(T_x)\,dx$, where 2 is a factor that takes into account the two outmost single layers of a multilayered GNR, w is a nanoribbon width, and $J_{PAEE}(T_x)$ is the phonon-assisted emission current density from the surface of a single-walled CNT with circumference equal to the width of the nanoribbon at temperature T_x. For a given GNR with fixed R_c, R_{th}, and k_0, $J_{PAEE}(T_x)$ is determined by the applied V_{pump} and, correspondingly, I_{pump}.[15] The details of $J_{PAEE}(T_x)$ calculation are referred to ref 15. Figure 4b presents the theoretical fitting of the experimental $I_{collect}-V_{pump}$ curve in

Figure 2d according to the PAEE model, and the required average temperature of the GNR corresponding to the theoretical curve is shown in Figure 4a. It is evident that the experimental $I_{collect}-V_{pump}$ curves are well described by the PAEE model, and that the required temperatures are less than 1500 K, being much lower than those needed for thermionic emission. Therefore, phonon-assisted electron emission is thought to be responsible for the experimentally measured electron emission from GNRs. And the electrons were emitted (or mainly emitted) in a perpendicular way from atomic surfaces of GNRs, as shown in Figure 3b, rather than from their 1D edges.

The perpendicular way of electron emission from GNRs under an internal electrical drive is different from the widely studied field electron emission from graphenes, which takes place in a parallel way from their 1D edges.[1−10] The quite different ways of electron emission under different causes can be well understood by taking into account the 2D character of graphenes, which presume both sharp 1D edges and broad 2D atomic surfaces. For field emission, electrons are emitted under the pull of an external electric field. Since there is a higher field enhancement factor, and thus much higher local external electric field at the sharp 1D edges, as compared to those at broad 2D surfaces, field emission prefers to take place from the 1D edges. However, for the presently measured electron emission under the internal electric field drive, electrons are expected to be emitted with the same probability from all the boundaries between vacuum and graphene including its 1D edges and 2D surfaces (if there are the same work functions at those sites). Since 2D surfaces compose of almost all possible boundaries between vacuum and graphene, clearly its electrons will mainly escape from the 2D atomic surfaces under the regarded internal drive. Therefore, there are two ways for electron emission from a 2D solid, as shown in Figure 3, and which way dominates the electron emission depends on its driving source.

Emission current from an individual GNR can reach as high as 4.6 nA (Figure 2b), which corresponds to an average emission density as high as 12.7 A/cm^2. Such emission density is about 3 to 4 orders of magnitude higher than that of field emission from graphene films.[1−3] More importantly, such high emission density was achieved under a low driving voltage of only <3 V, 2 orders of magnitude less than that needed for field emission.[12] Moreover, the internally driving character makes the electron emission less sensitive to the graphene emitter micro/nanostructures, since the latter can only strongly influence the local strength of an external electric field, but not the internal one. An internally driven electron emitter can be fabricated by simply connecting a GNR to two electrodes, similar to a GNR transistor, so GNR electron emitters can rather easily be fabricated and integrated using current well-developed micro- or nanofabrication techniques. Finally, we envisage that high emission density, low working voltage, and internal driving character may bring to the forefront the real applications of electron emission from GNRs driven by an internal electric field.

CONCLUSION

Electron emission from individual GNRs driven by internal electric field was studied for the first time inside a high resolution TEM equipped with a state-of-art STM sample holder with individually manipulated twin probes. Electrons were driven out from individual GNRs under an internal driving voltage of less than 3 V (or a driving electric field of only $\sim 10^6$ V/m) with an emission current increasing exponentially with the driving voltage. The internal driving voltage or electric field was 2 or 3 orders of magnitude less than those needed for field emission. One-atom-thick graphene nature enables both parallel electron emission from its edges and perpendicular electron emission from its atomic surfaces. On the basis of the careful analysis of the experimental data by taking into account the monatomic thickness of GNRs, the electron emission from GNRs was attributed to the phonon-assisted emission mechanism and was found to take place perpendicularly to atomic graphene surfaces with an average emission density as high as 12.7 A/cm^2. The internal driving character results in less sensitivity to the micro- and/or nanostructures of the graphene emitters as compared to field emission. The low working voltage, high emission density, and internal field driving character make the regarded electron emission highly promising for immediate electron source applications.

METHODS

The experiments were performed *in situ* inside a 300 kV high resolution field emission TEM (JEM 3100FEF) equipped with a state-of-art sample holder (Nanofactory Instruments) with two independent piezo-tube driven manipulators. A chemically etched W nanoprobe was mounted to each manipulator to act as an electrical probe that can be moved in three dimensions with a nearly nanometer precision under the piezo-tubes' drives. GNRs were synthesized through an arc-discharge method[23] and were attached to the edge of an Au wire, which was fixed to the terminal facing the W probes (Figure 1b). Under TEM observations, an individual GNR protruding from the Au wire edge was first selected, and its structure was entirely characterized using high resolution TEM imaging and electron diffraction. Under the control of manipulators, the W nanoprobe was moved to contact with the free end of the GNR, then the second W probe was moved close to the middle of the GNR to work as an emission current collecting probe. The driving voltage (V_{pump}) and current (I_{pump}) were applied and measured using a controller designed by Nanofactory Instruments for the twin-probe holder, whereas

the collecting voltage ($V_{collect}$) and collected emission current ($I_{collect}$) were applied and measured with a Keithley source measurement unit (model 236). The electrical measurements were always performed when the electron beam of TEM was blanked in order to avoid secondary electrons emissions.

Acknowledgment. This work was supported by the International Center for Young Scientists (ICYS) and the International Center for Materials Nanoarchitectonics (MANA) of the National Institute for Materials Science (NIMS). X. L. Wei is indebted to Prof. Q. Chen and Prof. L.-M. Peng for valuable discussions.

Supporting Information Available: Additional electron emission characteristics measured from a representative 680 nm long and 35.3 nm wide GNR. This material is available free of charge *via* the Internet at http://pubs.acs.org.

REFERENCES AND NOTES

1. Wu, Z.-S.; Pei, S. F.; Ren, W. C.; Tang, D. M.; Gao, L. B.; Liu, B. L.; Li, F.; Liu, C.; Cheng, H. M. Field Emission of Single-Layer Graphene Films Prepared by Electrophoretic Deposition. *Adv. Mater.* **2009**, *21*, 1756–1760.
2. Huang, Q. S.; Wang, G.; Guo, L. W.; Jia, Y. P.; Lin, J. J.; Li, K.; Wang, W. J.; Chen, X. L. Approaching the Intrinsic Electron Field-Emission of a Graphene Film Consisting of Quasi-freestanding Graphene Strips. *Small* **2011**, *7*, 450–454.
3. Uppireddi, K.; Rao, C. V.; Ishikawa, Y.; Weiner, B. R.; Morell, G. Temporal Field Emission Current Stability and Fluctuations from Graphene Films. *Appl. Phys. Lett.* **2010**, *97*, 062106.
4. Palnitkar, U. A.; Kashid, R. V.; More, M. A.; Joag, D. S.; Panchakarla, L. S.; Rao, C. N. R. Remarkably Low Turn-on Field Emission in Undoped, Nitrogen-Doped, and Boron-Doped Graphene. *Appl. Phys. Lett.* **2010**, *97*, 063102.
5. Hojati-Talemi, P.; Simon, G. P. Field Emission Study of Graphene Nanowalls Prepared by Microwave-Plasma Method. *Carbon* **2011**, *49*, 2869–2877.
6. Soin, N.; Roy, S. S.; Roy, S.; Hazra, K. S.; Misra, D. S.; Lim, T. H.; Hetherington, C. J.; McLaughlin, J. A. Enhanced and Stable Field Emission from *in Situ* Nitrogen-Doped Few-Layered Graphene Nanoflakes. *J. Phys. Chem. C* **2011**, *115*, 5366–5372.
7. Xiao, Z. M.; She, J. C.; Deng, S. Z.; Tang, Z. K.; Li, Z. B.; Lu, J. M.; Xu, N. S. Field Electron Emission Characteristics and Physical Mechanism of Individual Single-Layer Graphene. *ACS Nano* **2010**, *4*, 6332–6336.
8. Santandrea, S.; Giubileo, F.; Grossi, V.; Santucci, S.; Passacantando, M.; Schroeder, T.; Lupina, G.; Di Bartolomeo, A. Field Emission from Single and Few-Layer Graphene Flakes. *Appl. Phys. Lett.* **2011**, *98*, 163109.
9. Lee, S. W.; Lee, S. S.; Yang, E.-H. A Study on Field Emission Characteristics of Planar Graphene Layers Obtained from a Highly Oriented Pyrolyzed Graphite Block. *Nanoscale Res. Lett.* **2009**, *4*, 1218–1221.
10. Huang, C.-K.; Ou, Y. X.; Bie, Y. Q.; Zhao, Q.; Yu, D. P. Well-Aligned Graphene Arrays for Field Emission Displays. *Appl. Phys. Lett.* **2011**, *98*, 263104.
11. Dolan, W. W.; Dyke, W. P. Temperature-and-Field Emission of Electrons from Metals. *Phys. Rev.* **1954**, *95*, 327–332.
12. Xu, N. S.; Ejaz Huq, S. Novel Cold Cathode Materials and Applications. *Mater. Sci. Eng. R* **2005**, *48*, 47–189.
13. De Jonge, N.; Bonard, J.-M. Carbon Nanotube Electron Sources and Applications. *Phil. Trans. R. Soc. London, A* **2004**, *362*, 2239–2266.
14. Wang, W. L.; Qin, X. Z.; Xu, N. S.; Li, Z. B. Field Electron Emission Characteristic of Graphene. *J. Appl. Phys.* **2011**, *109*, 044304.
15. Wei, X. L.; Golberg, D.; Chen, Q.; Bando, Y.; Peng, L. M. Phonon-Assisted Electron Emission from Individual Carbon Nanotubes. *Nano Lett.* **2011**, *11*, 734–739.
16. Liu, Z.; Suenaga, K.; Harris, P. J. F.; Iijima, S. Open and Closed Edges of Graphene Layers. *Phys. Rev. Lett.* **2009**, *102*, 015501.
17. Chopra, N. G.; Benedict, L. X.; Crespi, V. H.; Cohen, M. L.; Louie, S. G.; Zettl, A. Fully Collapsed Carbon Nanotubes. *Nature* **1995**, *377*, 135–138.
18. Becker, J. A. Thermionic Electron Emission and Adsorption (Part I. Thermionic Emission). *Rev. Mod. Phys.* **1935**, *7*, 95–128.
19. O'Dwyer, M. F.; Lewis, R. A.; Zhang, C. Thermionic Refrigeration in Low-Dimensional Structures. *Microelectron. J.* **2008**, *39*, 597–600.
20. Yan, Q. M.; Huang, B.; Yu, J.; Zheng, F. W.; Zang, J.; Wu, J.; Gu, B.-L.; Liu, F.; Duan, W. H. Intrinsic Current−Voltage Characteristics of Graphene Nanoribbon Transistors and Effect of Edge Doping. *Nano Lett.* **2007**, *7*, 1469–1473.
21. Campos-Delgalo, J.; Kim, Y. A.; Hayashi, T.; Morelos-Gomez, A.; Hofmann, M.; Muramatsu, H.; Endo, M.; Terrones, H.; Shull, R. D.; Dresselhaus, M. S.; *et al.* Thermal Stability Studies of CVD-Grown Graphene Nanoribbons: Defect Annealing and Loop Formation. *Chem. Phys. Lett.* **2009**, *469*, 177–182.
22. Huang, X. Y.; Zhang, Z. Y.; Liu, Y.; Peng, L. M. Analytical Analysis of Heat Conduction in a Suspended One-Dimensional Object. *Appl. Phys. Lett.* **2009**, *95*, 143109.
23. Ando, Y.; Iijima, S. Preparation of Carbon Nanotubes by Arc-Discharge Evaporation. *Jpn. J. Appl. Phys.* **1993**, *32*, L107–L109.